X-ray Crystallographic Studies of Unique Cross-Linked Lattices between Four Isomeric Biantennary Oligosaccharides and Soybean Agglutinin[†,‡]

Laurence R. Olsen,[§] Andréa Dessen,[§,||] Dipti Gupta,[⊥,#] Subramaniam Sabesan,[○] James C. Sacchettini,*[,§,△] and C. Fred Brewer*[,⊥]

Departments of Biochemistry and Molecular Pharmacology, Microbiology and Immunology, Albert Einstein College of Medicine, Bronx, New York 10461, and Du Pont Company, Wilmington, Delaware 19880-0328

Received July 28, 1997; Revised Manuscript Received September 26, 1997[⊗]

ABSTRACT: Soybean agglutinin (SBA) (*Glycine max*) is a tetrameric GalNAc/Gal-specific lectin which forms unique cross-linked complexes with a series of naturally occurring and synthetic multiantennary carbohydrates with terminal GalNAc or Gal residues [Gupta *et al*. (1994) *Biochemistry 33,* 7495−7504]. We recently reported the X-ray crystal structure of SBA cross-linked with a biantennary analog of the blood group I carbohydrate antigen [Dessen *et al*. (1995) *Biochemistry 34*, 4933−4942]. In order to determine the molecular basis of different carbohydrate−lectin cross-linked lattices, a comparison has been made of the X-ray crystallographic structures of SBA cross-linked with four isomeric analogs of the biantennary blood group I carbohydrate antigen. The four pentasaccharides possess the common structure of (β-LacNAc)$_2$Gal-β-R, where R is $-O(CH_2)_5COOCH_3$. The β-LacNAc moieties in the four carbohydrates are linked to the 2,3-, 2,4-, 3,6-, and 2,6-positions of the core Gal residue(s), respectively. The structures of all four complexes have been refined to approximately 2.4−2.8 Å. Noncovalent lattice formation in all four complexes is promoted uniquely by the bridging action of the two arms of each bivalent carbohydrate. Association between SBA tetramers involves binding of the terminal Gal residues of the pentasaccharides at identical sites in each monomer, with the sugar(s) cross-linking to a symmetry-related neighbor molecule. While the 2,4-, 3,6-, and 2,6-pentasaccharide complexes possess a common $P6_422$ space group, their unit cell dimensions differ. The 2,3-pentasaccharide cross-linked complex, on the other hand, possesses the space group $I4_122$. Thus, all four complexes are crystallographically distinct. The four cross-linking carbohydrates are in similar conformations, possessing a pseudo-2-fold axis of symmetry which lies on a crystallographic 2-fold axis of symmetry in each lattice. In the case of the 3,6- and 2,6-pentasaccharides, the symmetry of their cross-linked lattices requires different rotamer orientations about their β(1,6) glycosidic bonds. The results demonstrate that crystal packing interactions are the molecular basis for the formation of distinct cross-linked lattices between SBA and four isomeric pentasaccharides. The present findings are discussed in terms of lectins forming unique cross-linked complexes with glycoconjugate receptors in biological systems.

Lectins are carbohydrate binding proteins that are widely distributed in nature, including in microorganisms, plants, and animals (*1*). Lectins with similar specificities and protein folding patterns are conserved in nematodes, vertebrates, and plants, suggesting the importance of their biological functions (cf. refs 2, 3). In fact, the biological roles of animal lectins have been established in many cases. A number of mammalian lectins are involved in receptor-mediated endocytosis of glycoproteins (cf. ref 4), while others have been implicated in cellular recognition processes including adhesion (*4*), metastasis (*5*, *6*), and apoptosis (*7*).

A common structure−activity property of most lectins is their multivalent carbohydrate binding activities. The X-ray crystal structures of many plant and animal lectins confirm their oligomeric structures (cf. refs 2, 8). As a consequence of their multivalency, lectin binding to cells often leads to cross-linking and aggregation of specific glycoproteins and glycolipids receptors, which, in many cases, is associated with signal transduction effects. For example, cross-linking of cell surface glycoconjugates has been implicated in the mitogenic activities of lectins (*9*), in the arrest of bulk transport in ganglion cell axons (*10*), in the induction of mating reactions in fungi (*11*), in the molecular sorting of glycoproteins in the secretory pathways of cells (*12*), and in the apoptosis of activated human T-cells (*7*). Furthermore, lectin-induced cross-linking of cellular

[†] This work was supported, in part, by Grant CA-16054 from the National Cancer Institute, Department of Health, Education, and Welfare, Core Grant P30 CA-13330 from the same agency (C.F.B.), Grants GM-47637 and GM-45859 from the National Institute of General Medical Sciences, and the Welch Foundation (J.C.S.). A.D. was supported by a postdoctoral fellowship from the Heiser Foundation. L.R.O. was supported by a postdoctoral fellowship from the Aaron Diamond Foundation.

[‡] Coordinates for the crystal structures of the soybean agglutinin cross-linked with the 2,3-, 2,4-, and 3,6-pentasaccharides have been deposited with the Brookhaven Protein Data Bank as 1SBF, 1SBD, and 1SBE, respectively.

* To whom correspondence should be addressed.

[§] Department of Biochemistry, Albert Einstein College of Medicine.

[||] Present address: Laboratory of Molecular Medicine, The Children's Hospital, Boston, MA 02115.

[⊥] Department of Molecular Pharmacology, Microbiology and Immunology, Albert Einstein College of Medicine.

[#] Present address: Smithkline Beecham Pharmaceuticals, King of Prussia, PA 19406.

[○] Du Pont Company.

[△] Present address: Department of Biochemistry and Biophysics, Texas A&M University, College Station, TX 77843.

[⊗] Abstract published in *Advance ACS Abstracts,* December 1, 1997.

S0006-2960(97)01828-X CCC: $14.00

transmembrane glycoproteins leads to changes in their interactions with cytoskeletal proteins and concomitant alterations in the mobility and aggregation of other surface receptors (*13*, *14*). Thus, the carbohydrate cross-linking properties of lectins appear to be a key feature of their biological activities.

Insights into lectin−carbohydrate cross-linking interactions have been obtained by investigating the binding of lectins to the oligosaccharide chains of glycoproteins and glycolipids. Many of these branch-chain oligosaccharides have been shown to be multivalent and to bind, cross-link, and precipitate with specific multivalent lectins (*15*−*20*). Importantly, these interactions lead to the formation of homogeneous cross-linked complexes between lectins and oligosaccharides and glycopeptides (*20*−*23*). For example, quantitative precipitation studies of binary mixtures of a series of oligomannose glycopeptides and a bisected hybrid-type glycopeptide with the Glc/Man-specific lectin, ConA,[1] indicate that each glycopeptide forms unique, homogeneous cross-linked complexes with the lectin (*21*). Complexes containing different glycopeptides bound to a single lectin molecule fail to precipitate. Similar studies have shown that mixtures of complex-type oligosaccharides and several Gal-specific lectins including SBA also form homogeneous cross-linked complexes (*23*).

The ability of lectins to form homogeneous cross-linked complexes with multivalent carbohydrates has been shown to be due to the formation of highly ordered, unique cross-linked lattices. For example, the precipitates formed between the Fuc-specific isolectin A from *Lotus tetragonolobus* (LTL-A) and three structurally related biantennary fucosyl oligosaccharides show distinct, highly organized cross-linked lattices for each carbohydrate when viewed by negative stain or freeze fracture electron microscopy (EM) (*20*). Similar observations have been made of the cross-linked complexes formed between the Gal/GalNAc-specific plant lectin SBA and a variety of naturally occurring and synthetic multiantennary oligosaccharides with terminal Gal or GalNAc residues including a series of blood group I antigen analogs (*24*). Mixed quantitative precipitation experiments suggested unique cross-linked complexes between the carbohydrates and SBA, while negative stain EM images indicated the formation of highly ordered cross-linked lattices in many instances (*24*).

Recently, the structure of SBA cross-linked with an analog of the blood group I carbohydrate antigen (2,6-pentasaccharide in Figure 1) has been determined by X-ray crystallography at a resolution of 2.6 Å (*25*). The structure shows that lattice formation is promoted uniquely by the bridging action of the bivalent pentasaccharide. Association between tetramers of SBA involves binding of the terminal Gal residues of the pentasaccharide at identical sites in each protein monomer, with the sugar cross-linking to a symmetry-related neighbor molecule. However, while the structural role of the cross-linking carbohydrate is clear in the case of the 2,6-pentasaccharide complex, the structural basis for the formation of different cross-linked complexes between SBA and other related carbohydrates is the subject of the present investigation.

[1] Abbreviations: SBA, lectin from soybean (*Glycine max*); ConA, lectin from jack bean (*Canavalia ensiformis*); N-linked, asparagine-linked; LacNAc, Galβ(1,4)GlcNAc; NMR, nuclear magnetic resonance; EM, electron microscopy. All sugars are in the D-configuration.

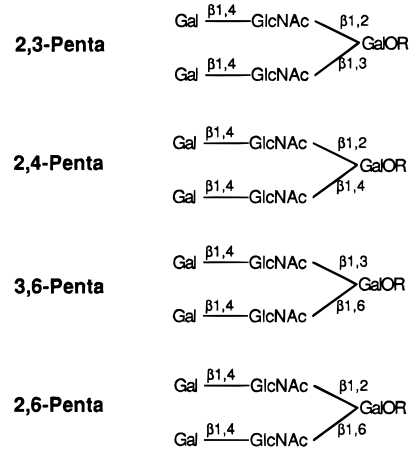

FIGURE 1: Structures of the 2,3-, 2,4-, 3,6-, and 2,6-pentasaccharides. The aglycon moiety R is $-(CH_2)_5COOCH_3$. The core galactose residue is in the β-anomeric configuration.

The present study compares the crystal structures of SBA cross-linked with four isomeric analogs of the blood group I antigen (Figure 1) as determined by X-ray diffraction analysis. While complexes between SBA and 2,4-, 3,6-, and 2,6-pentasaccharides yield crystals belonging to the same space group, the variations in unit cell dimensions reveal differences that provide the molecular basis of the unique cross-linked lattices of the carbohydrates with the lectin. The more acute angle relating the arms of the 2,3-pentasaccharide results in a crystalline lattice belonging to a space group distinct from the other three sugar−lectin complexes and serves to emphasize the unique role of the bivalent sugars in mediating lattice formation. The results thus provide a molecular basis for the formation of unique, homogeneous cross-linked complexes between a single lectin and a series of structurally related bivalent oligosaccharides. In turn, this provides a mechanism for the formation of selective, clustered arrays of lectin−glycoconjugate receptors in biological systems.

MATERIALS AND METHODS

The four carbohydrates in Figure 1 were synthesized as previously described (*26*). The purity of the oligosaccharides was confirmed by ^{1}H NMR. Native SBA was purified as previously described (*17*).

Crystallization. The four SBA−pentasaccharide complexes were crystallized by the hanging drop vapor diffusion method, as previously described (*25*). Single crystals of up to 3.0 mm on each edge could be grown with this method. Crystals of the 2,4- and 3,6-pentasaccharide complexes crystallized in space group $P6_422$, which was the same as for the 2,6-pentasaccharide complex previously described (*25*). Crystals of the 2,3-pentasaccharide complex crystallized in space group $I4_122$. Unit cell parameters for all four complexes are given in Table 1.

Data Collection. X-ray diffraction data were collected on a Siemens area detector system coupled to a Rigaku RU-200 rotating anode X-ray generator. The data were processed with the XENGEN software package (Siemens Analytical X-ray Instruments, Inc., Madison, WI) (*27*). Table 2 gives a summary of the data collection and data reduction parameters for all four crystalline complexes.

Structure and Refinement. The structure of SBA bound to the 2,6-pentasaccharide (*25*) was used to solve the

Table 1: Space Group and Unit Cell Parameters of SBA Cross-Linked with the 2,3-, 2,4-, 3,6-, and 2,6-Pentasaccharides

complex	space group	*a* (Å)	*b* (Å)	*c* (Å)	α (deg)	*β* (deg)	*γ* (deg)
SBA−2,3-pentasaccharide	$I4_122$	122.6	122.6	90.6	90	90	90
SBA−2,4-pentasaccharide	$P6_422$	144.6	144.6	107.2	90	90	120
SBA−3,6-pentasaccharide	$P6_422$	143.3	143.3	107.8	90	90	120
SBA−2,6-pentasaccharide	$P6_422$	144.9	144.9	109.4	90	90	120

Table 2: Data Collection and Reduction for SBA Cross-Linked Carbohydrate Complexes

	SBA−2,3[a]	SBA−2,4[b]	SBA−3,6[c]
scan width	0.25	0.25	0.25
resolution limits (Å)	2.43	2.52	2.80
no. of observations	57894	112590	61134
no. of unique reflections	12224	19406	16633
redundancy	4.74	5.80	3.73
mean $Y/\sigma I$	13.9	15.8	4.1
R_{sym} on intensity (%)	12.8	14.0	13.9
R_{sym} on intensity in last resolution shell	30	41	54
completeness of data (%)	91	85	84
completeness of data (%) in last resolution shell	85	49	67

[a] 2,3-Pentasaccharide−SBA complex. [b] 2,4-Pentasaccharide−SBA complex. [c] 3,6-Pentasaccharide−SBA complex.

structure of the 2,4- and 3,6-pentasaccharide complexes. Since all three of these complexes crystallized in space group $P6_422$, molecular replacement was not required to solve the other two structures. Rather, each was first submitted to rigid-body refinement using X-PLOR (*28*). *R*-factors of 24% and 30% were thus obtained for the 2,4- and 3,6-pentasaccharide complex structures, respectively. Refinement of the two structures was then continued by using the rigid-body minimized model. The process of refining the starting model for each structure was divided into several macrocycles, each of which involved manual rebuilding of the model using the program TOM (*29*), displayed on a Silicon Graphics workstation. "Omit" maps were employed in model building and used to modify areas of poor geometry. Manually adjusted models were refined using the least-squares positional refinement algorithm of TNT (*30*). Refinement and model building were judged to be complete when no further assignable density was apparent on $|F_o| - |F_c|$ maps and no further reduction in *R*-factor could be produced without deleterious effects on the geometry. In a final stage of refinement, advantage was made of the superior quality of the data for the 2,3-pentasaccharide complex. A matrix was calculated using the TNT program OVERLAY which superimposed the Cα backbone of the 2,3-pentasaccharide complex onto that for the 2,4 or the 3,6 complexes. The models, which contained all protein atoms for which density was unambiguous for both the complex being fitted and the 2,3-pentasaccharide complex model, were put into the 2,4 or 3,6 complex's unit cell and used as targets for simulated annealing using the X-PLOR routine SLOWCOOL with an initial temperature of 3000 K. All 12−2.52 and 8.0−2.8 Å data were used to refine the 3,6 complex and the 2,4 complex, respectively. Simulated annealing (4000 K) omit maps for each 10 residues were also calculated to assist in map interpretation and prevent the incorporation of model bias into the rebuilt models for the 2,4 and 3,6 complexes. Use of the simulated-annealed models in conjunction with the omit maps for the 2,4 and 3,6 complexes resulted in improved model clarity, especially for loop regions. Missing side chains and waters were built into the new models where there was clear density in omit maps for them. The final models for the 2,4-pentasaccharide and 3,6-pentasaccharide complexes had *R*-factors of 20.5% and 21.0% and included 45 and 20 waters, respectively. The 2,4-pentasaccharide model has final rms bond length deviations of 0.017 Å and rms bond angle deviations of 2.34°. The corresponding numbers for the 3,6-pentasaccharide model are 0.013 Å and 2.50°. Due to the absence of electron density, the region from Ser116 to Asp118 is not included in the 3,6 model. Residues Ser116 and Gly117 are not included in the 2,4 model. Residues with poor electron density for their side chains are modeled as alanine. All models include a cis-peptide bond between Ala87 and Asp88 as found in all legume lectins (cf. refs 31, 32).

The structure of the 2,3-pentasaccharide complex was solved by molecular replacement using the protein portion of the 2,6-sugar complex as the search model. Cross-rotation and subsequent translation functions were calculated using AMORE (*33*). The rotation angles and translation functions calculated on 8−5 Å data yielded a solution at 10.6σ above the mean and an initial *R*-factor of 40%, with the next best peak being 4.4σ above the mean. The rotated and translated model was then rigid-body refined using X-PLOR, which reduced the *R*-factor to 31%. At this point 10% of the data was randomly chosen for calculation of *R*-free. The *R*-free decreased in all subsequent X-PLOR refinement steps. Application of simulated annealing and individual *B*-factor refinement reduced the *R*-factor to 23.3% (*R*-free = 33%). The calculated maps were of sufficient quality to allow manual incorporation of the two terminal sugars from the noncovalent saccharide, as well as the two divalent metal ions and their water ligands. Another round of simulated annealing reduced the *R*-factor to 22%, at which point multiple rounds of model building using the program O (*34*) and positional refinement with the program TNT improved the model to its final *R*-factor of 18.7% with rms bond length and bond angle deviations of 0.011Å and 1.9°, respectively. The final model contains 22 water molecules.

RESULTS AND DISCUSSION

Protein Structure. Examination of the Cα coordinates of SBA in the cross-linked complexes with the 2,3-, 2,4-, and 3,6-pentasaccharides shows that the coordinates are similar to one another as well as to the structure of the lectin in the 2,6-pentasaccharide complex (*25*). The Cα coordinates of SBA in the 2,3- and 3,6-pentasaccharide complexes, for example, can be almost perfectly superimposed (Figure 2). The root mean square (rms) differences between pairs of Cα positions for the four structures are listed in Table 3. The superimposed structures in Figure 2 show that the main differences lie in the loop areas, the major secondary structural elements being nearly identical. The polypeptide fold consists of two separate sheets of antiparallel *β*-strands. There are six *β*-strands in the first sheet, and seven in the

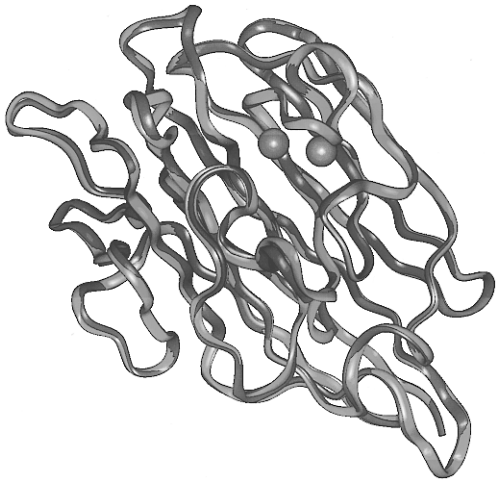

FIGURE 2: Superimposed Cα coordinates of SBA for the cross-linked complexes with the 2,3- and 3,6-pentasaccharides (blue and red, respectively) in Figure 1. The Mn^{2+} and Ca^{2+} ions in the protein are designated by green and magenta balls, respectively. The root mean square (rms) differences between each pair of structures were measured by calculating the rms difference between Cα positions of both structures (Insight II) and are given in Table 3. The superimposed structures reveal that the main differences lie in the loop areas, the major secondary structural elements being nearly identical.

sheet which provides the framework for support of the metal binding region (β-sheet II), as has been previously described for SBA bound to the 2,6-pentasaccharide (*25*). This framework is common for legume lectins as well as certain animal lectins (cf. refs 2, 32, 35).

Table 3: RMS Difference between Cα Positions of SBA−Pentasaccharide Structures

complex	complex	rms (Å)
SBA−2,3[a]	SBA−2,4[b]	0.341
SBA−2,3[a]	SBA−2,6[d]	0.368
SBA−2,3[a]	SBA−3,6[c]	0.383
SBA−2,4[b]	SBA−2,6[d]	0.275
SBA−2,4[b]	SBA−3,6[c]	0.328
SBA−2,6[d]	SBA−3,6[c]	0.349

[a] 2,3-Pentasaccharide−SBA complex. [b] 2,4-Pentasaccharide−SBA complex. [c] 3,6-Pentasaccharide−SBA complex. [d] 2,6-Pentasaccharide−SBA complex.

Nearly all of the amino acids in the three structures have ϕ and ψ angles that fall within energetically allowed regions of the Ramachandran plot. Two exceptions for all structures are Asp88 and Asn136. Asn159 is also in an unfavorable region in the models for the 2,4- and the 3,6-pentasaccharide complexes. Asp88 is involved in a cis-peptide bond conserved among lectins (cf. refs 31, 32). Asn136 and 159 are in surface loops, and their poor geometry is enforced by numerous hydrogen bond interactions with neighboring residues. The only remaining area of poor geometry is in or near the loop encompassing residues 112−119. Portions of this loop are not included in the models for the 2,4- and the 3,6-pentasaccharide complexes because of weak electron density.

Protein−Carbohydrate Contacts and Conformations of the Bound Pentasaccharides. In all four cross-linked complexes, the two LacNAc arms of each carbohydrate are symmetrically related by a crystallographic 2-fold axis through

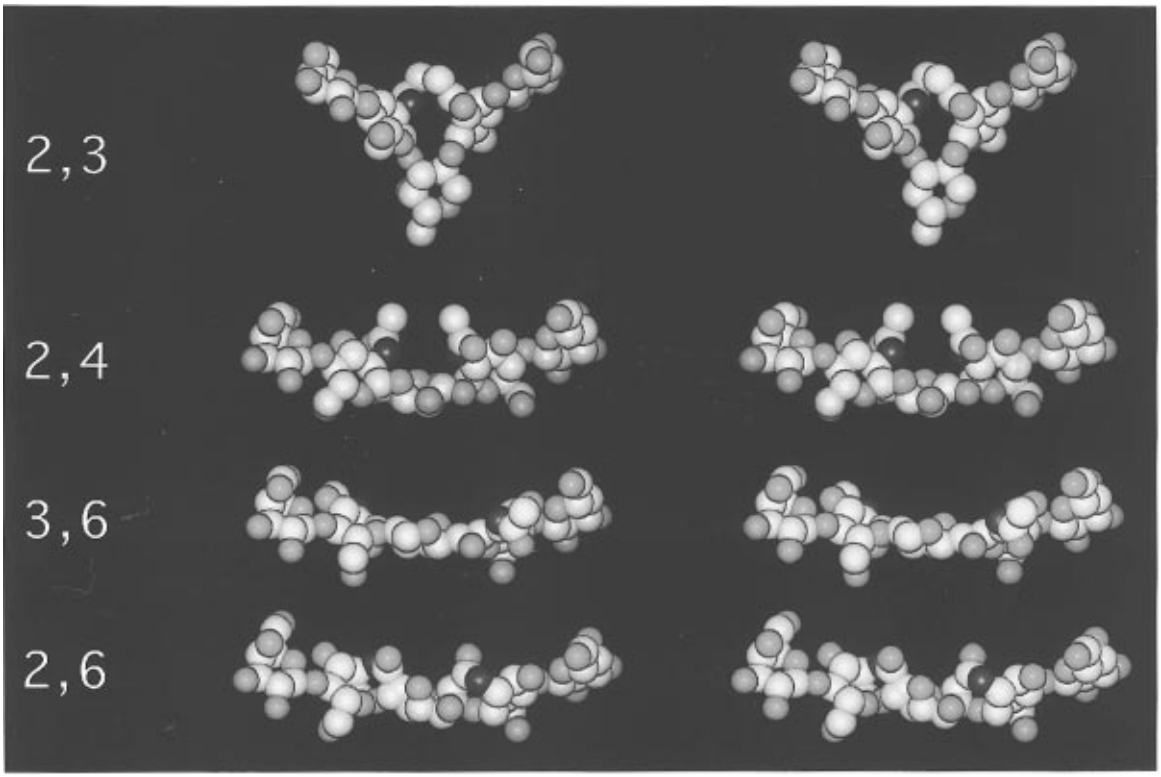

FIGURE 3: Conformations of the bound 2,3-, 2,4-, 3,6-, and 2,6-pentasaccharides shown as stereo CPK models in their respective cross-linked complexes with SBA. For clarity purposes, the core Gal residue in each oligosaccharide is shown in one of two nonsymmetric orientations, while the outer two LacNAc residues are related to each other by 2-fold symmetry. The β(1,6) arm of the 3,6-pentasaccharide oligosaccharide is bound in the $\omega = 60°$ (gt) conformation, while the β(1,6) arm of the 2,6-pentasaccharide oligosaccharide is bound in the $\omega = -60°$ (gg) conformation. The dihedral angle ω is defined by O-5, C-5, C-6, and O-6. The core Gal residue was manually positioned into the structure for each complex on the basis of the electron density map for one of its two orientations. O1 of the core Gal is not shown, since C1 is bound to the aglycon moiety. These figures were generated with Insight.

Table 4: Glycosidic Torsion Angles ϕ, ψ for the LacNAc Residues of the Pentasaccharides in Their Cross-Linked Complexes with SBA and Distances between C6 Atoms of the Terminal Gal Residues between Symmetry-Related Cross-Linked Monomers

complex	ϕ (O-5, C-1, O-4′, C-4′) (deg)	ψ (C-1, O-4′, C-4′, C-5′) (deg)	distance (Å)
SBA−2,3[a]	−91	−135	15.0
SBA−2,4[b]	−127	−89	19.2
SBA−3,6[c]	−97	−129	19.7
SBA−2,6[d]	−87	−130	20.6

[a] 2,3-Pentasaccharide−SBA complex. [b] 2,4-Pentasaccharide−SBA complex. [c] 3,6-Pentasaccharide−SBA complex.

the core Gal residue. All four pentasaccharides therefore possess a pseudo-2-fold axis of symmetry in their respective complexes since the core Gal residue in each oligosaccharide lacks 2-fold symmetry (*24*). This is reflected in the poor electron density maps for the central Gal residue in each case. However, the LacNAc arms of the carbohydrates in all four complexes are well defined and establish the conformation of the cross-linking oligosaccharides.

All four pentasaccharides possess essentially the same carbohydrate−protein contacts in the binding site of SBA. These interactions have been described before in detail for the 2,6-pentasaccharide complex (*25*). Further refinement of the 2,6-pentasaccharide−SBA complex as well as the other three complexes has changed the assignment of hydrogen bonding of the Gal O-3 from O Ala105 to NH Gly106.

Figure 3 shows space-filling models (CPK) of the four carbohydrates in their cross-linked complexes. As can be seen, the relative conformations of the 2,4-, 3,6-, and 2,6-pentasaccharides are very similar. The terminal Gal moieties of the 2,4- and 3,6-carbohydrates are bound in the SBA binding site in approximately the same orientation as the Gal residues of the 2,6-pentasaccharide previously described (*25*) (Figure 2). Figure 3 also shows that the orientations of the β-LacNAc arms of the 2,3-pentasaccharide are at a more acute angle than those of the other three carbohydrates.

Values of the ϕ, ψ torsion angles for the $\beta(1-4)$ glycosidic bond in the Gal$\beta(1-4)$GlcNAc (LacNAc) linkage (defined as ϕ = O-5, C-1, O-4′, C-4′; ψ = C-1, O-4′, C-4′, C-5′) for the four pentasaccharide complexes are given in Table 4. The ϕ, ψ values for the LacNAc residues of the 2,3-, 3,6-, and 2,6-pentasaccharides are similar to those reported for LacNAc bound to the Gal-specific 14 kDa bovine spleen lectin (*36*). The ϕ, ψ values for the Gal$\beta(1-4)$GlcNAc linkage in the 2,3-pentasaccharide are similar to those of the 2,6-pentasaccharide. Differences in the ϕ, ψ angles for the 2,4-pentasaccharides appear to be due to the different core Gal linkages, as well as the constrained binding geometry of the outer Gal residues in the cross-linked complex. The ϕ, ψ angles for the Gal$\beta(1-4)$GlcNAc linkages in all four carbohydrates are within the torsion angle range reported for the disaccharide (*37*).

The rotationally flexible $\beta(1,6)$ arm of the bound 2,6-pentasaccharide has previously been assigned to the $\omega = -60°$ (gg) conformation (*25*), where ω is the dihedral angle defined by O-5, C-5, C-6, and O-6 (cf. ref 38). In this conformation, the two LacNAc arms are symmetrically related by a crystallographic 2-fold axis through the core Gal residue. However, this is the least energetically favorable of the three allowed rotamer populations around the β-(1,6) of the pentasaccharide by $\sim$1−2 kcal mol^{-1} (*26*). In the case of the 3,6-pentasaccharide, the $\beta(1,6)$ arm of the core galactose is fixed in the more stable "gt" orientation ($\omega = 60°$), based on the following. As can be seen from Figure 3, both the LacNAc residues in the cross-linked complexes of 2,6- and 3,6-pentasaccharides with the lectin are in similar positions with a pseudo-2-fold axis of symmetry about the crystallographic axis. This is despite the opposite geometry of the 2- and 3-hydroxyls of the core galactose which places the LacNAc units connected to these secondary hydroxyls in the 2,6- and 3,6-carbohydrates in opposite orientations. Therefore, the only way for the 3,6-pentasaccharide to exhibit the observed 2-fold axis of symmetry similar to the 2,6-pentasaccharide is to have its $\beta(1,6)$ arm of the core galactose in the gt orientation ($\omega = 60°$, Figure 4). Thus, crystal packing constraints in the cross-linked lattices require different rotamer orientations of the $\beta(1,6)$ arms of the 2,6- and 3,6-pentasaccharides. This suggests that the rotation flexibility of the $\beta(1,6)$ arms in these carbohydrates is an important structural determinant for their cross-linking interactions with SBA. Indeed, the $\beta(1,6)$ arm of a biantennary complex type carbohydrate with a terminal Gal residue has been observed to exist in three different rotamer orientations in crystalline cross-linked complexes with a Gal-specific 14 kDa animal lectin (*39*).

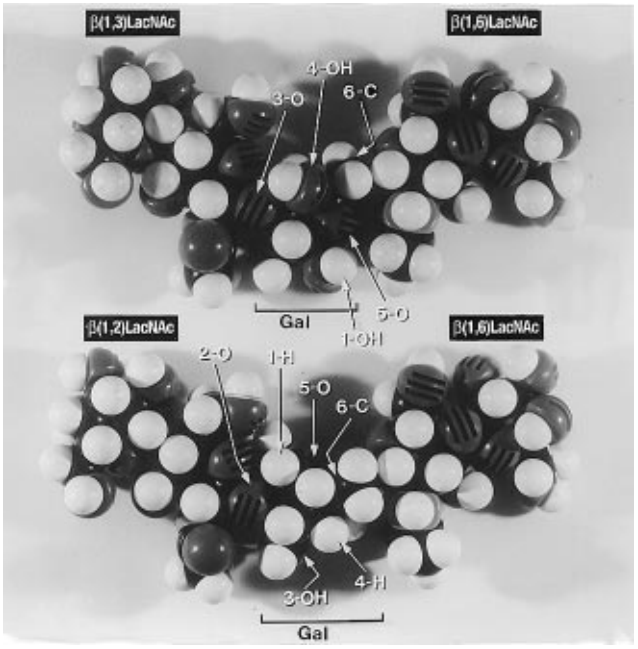

FIGURE 4: CPK models of the 3,6- (top) and 2,6-pentasaccharides (bottom) in their respective cross-linked complexes. The LacNAc residues of the 3,6- and 2,6-carbohydrates are in similar positions in the respective cross-linked complexes. The $\beta(1,3)$-linked LacNAc residue of the 3,6-pentasaccharide and the $\beta(1,2)$-linked LacNAc residue of the 2,6-pentasaccharide are on opposite sides of the core Gal residue due to differences in the configuration of the hydroxyl groups at the 2- and 3-positions of Gal. Since these two LacNAc arms in the 2,6- and 3,6-pentasaccharides are in similar orientations in their respective cross-linked lattices (Figure 3), the $\beta(1,6)$ arms for each oligosaccharide must be on opposite sides of the core Gal residue ($\omega = -60°$ and 60°, respectively) in order to provide the same pseudo-2-fold axis of symmetry for the two carbohydrates.

Lattice Structures. Table 1 shows the space group and unit cell dimensions of all four cross-linked complexes. While the 2,4-, 3,6-, and 2,6-pentasaccharide−SBA lattices belong to the same space group ($P6_422$), they manifest distinct differences in their unit cell dimensions. The 2,4-

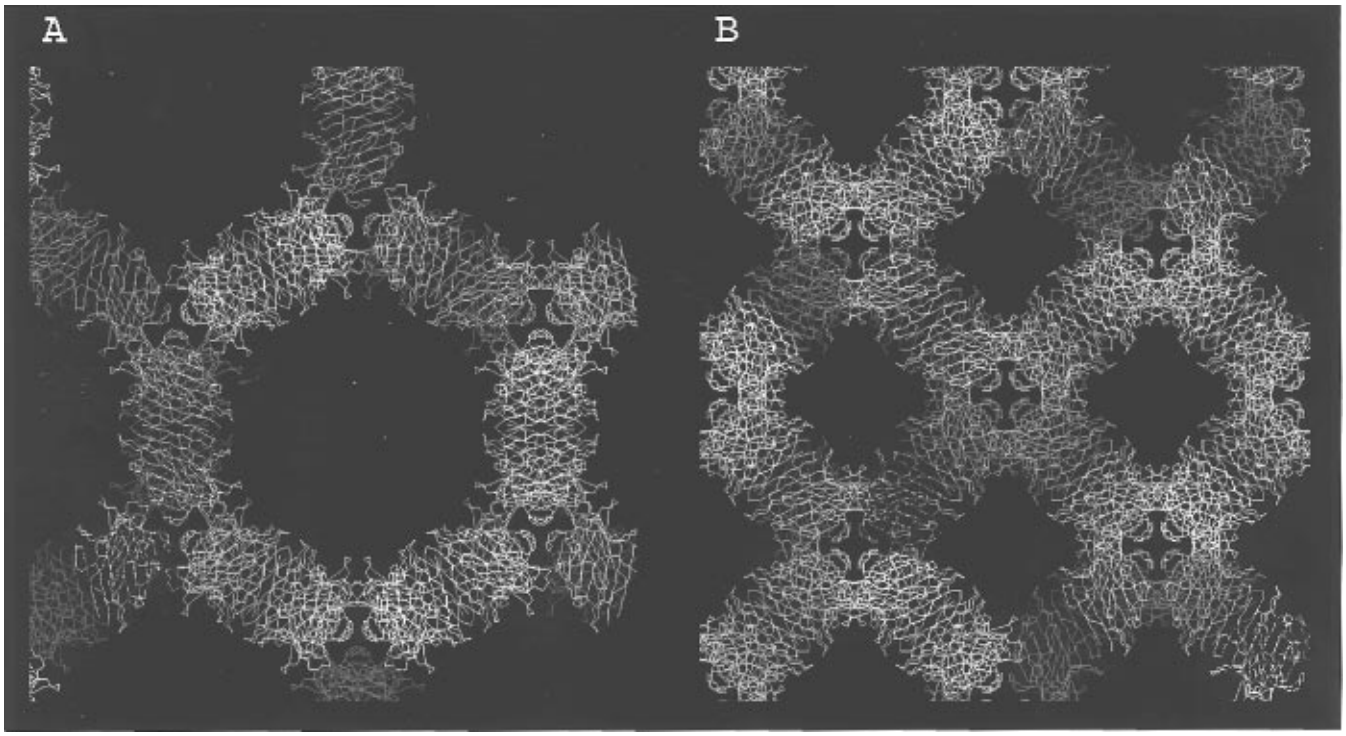

FIGURE 5: (A) The 6-fold axis of symmetry down the *c*-axis is shown for the 3,6-pentasaccharide cross-linked complex with SBA, and (B) the 4-fold axis of symmetry down the *c*-axis is shown for the 2,3-pentasaccharide cross-linked complex with SBA. In these views, protein molecules are shown as colored trace models (monomers), with the cross-linking oligosaccharides not shown. These figures were generated with MOLPACK.

and 2,6-pentasaccharide lattices exhibit small differences (0.3 Å) along their *a* and *b* axes, with a larger difference (2.2 Å) along the *c* axes. The 3,6-pentasaccharide lattice differs from the other two lattices along the *a* and *b* axes (1.3−1.6 Å). The lattice of the 3,6-pentasaccharide−SBA complex also differs along the *c* axis by 0.6 Å relative to the lattice of the 2,4-pentasaccharide−SBA complex. Differences in the *c* axes of all three lattices can be related to the distances separating the C-6 carbon atoms of the terminal Gal residues of each cross-linking pentasaccharide in symmetry-related SBA monomers. The distances of 19.2, 19.7, and 20.6 Å (Table 4) that separate the C-6 atoms of the terminal Gal residues of the 2,4-, 3,6-, and 2,6-pentasaccharides, respectively, correlate with the order of the distances along the *c* axes for all three complexes of 107.2, 107.8, and 109.4 Å (Table 1), respectively. Thus, the *c* axes of the three complexes reflect differences in lengths of the three carbohydrates.

In the case of the 2,3-pentasaccharide, the distance between the C-6 atoms of the terminal Gal residues is 15.0 Å, which is considerably shorter than the respective distances of the other three carbohydrates (Table 3). More importantly, the angle between the β-LacNAc arms is sufficiently acute to force the lattice to adopt a different space group ($I4_122$). Differences in the structure of the 2,3-pentasaccharide−SBA lattice relative to the other three complexes can be observed in Figure 5. The crystal lattices of the 2,4-, 3,6-, and 2,6-pentasaccharide−SBA complexes possess a common 6-fold axis of symmetry, which is shown for the 3,6-pentasaccharide complex in Figure 5A. In this view, the cross-linking oligosaccharide is not shown. A salient feature of the lattice(s) is the absence of a high degree of strong protein−protein contacts and formation of large, solvent-filled cavities (∼70%). By comparison, the 2,3-pentasaccharide complex (from nearly the same perspective) shows a 4-fold axis of symmetry, as shown in Figure 5B. The 4-fold axis of symmetry results in a contracted lattice relative to the 6-fold symmetry lattices of the other three pentasaccharides. The diameter of the cavity shown in Figure 5B for the 2,3-pentasaccharide−SBA lattice is ∼45 Å, while the diameter of the cavity shown in Figure 5A for the 3,6-pentasaccharide−SBA lattice and other two lattices is ∼100 Å.

Further differences in the lattice structure of the 2,3-pentasaccharide complex relative to the other three complexes can be seen in Figure 6. The structure of the 3,6-pentasaccharide lattice in the *z* plane, perpendicular to a 2-fold axis of the tetramer, is shown in Figure 6B. An SBA tetramer in the center is shown cross-linked to four other SBA molecules (single subunits shown only) via four cross-linking oligosaccharide molecules. The structure of the 2,3-pentasaccharide complex from nearly the same perspective is shown in Figure 6A. This view shows that there is a greater angle and distance separating cross-linked SBA molecules in the 2,3-pentasaccharide complex (the separation between two monomers above and below the central tetramer in Figure 6A) relative to the other three complexes. There is also a different twist angle between cross-linked SBA molecules in the 2,3-pentasaccharide complex and a shorter distance separating directly cross-linked SBA molecules (indicated by the shorter distance between terminal Gal residues in Table 3). Thus, the greater acute angle between the two LacNAc residues of the 2,3-pentasaccharide and shorter distance between terminal Gal residues relative to the other carbohydrates are responsible for the change in space group of the 2,3-pentasaccharide−SBA lattice.

We have previously reported that a series of blood group I related isomeric oligosaccharides, including the four pentasaccharides in the present study, induce different cross-linked lattices with SBA, based on quantitative precipitation analysis and electron microscopy studies (*24*). The present

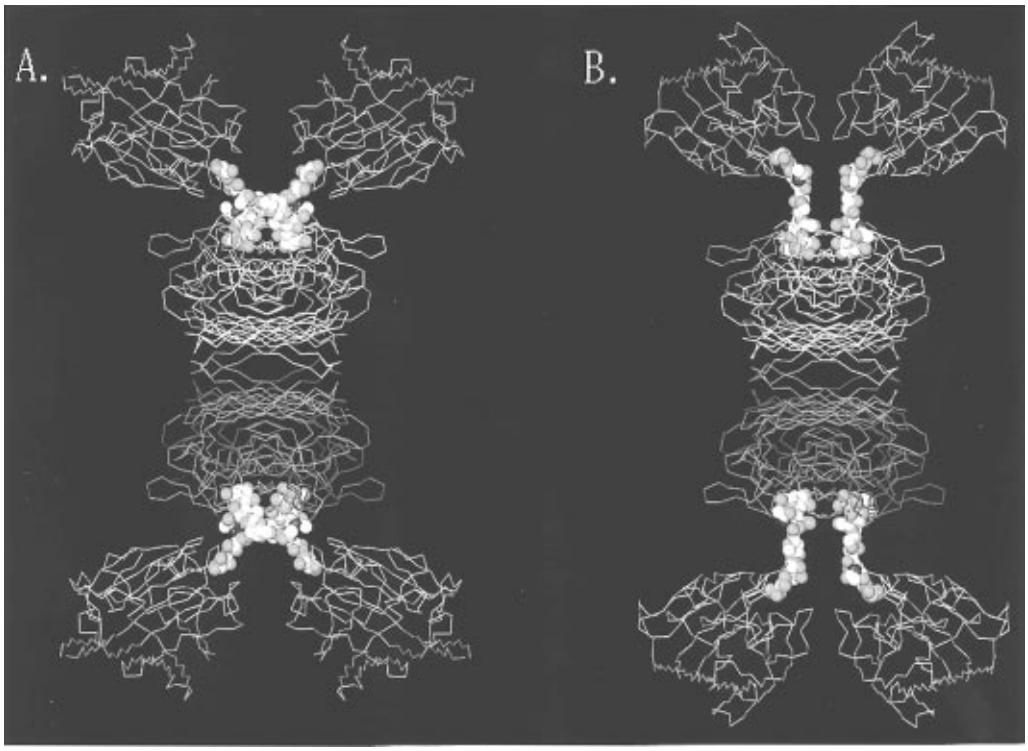

FIGURE 6: Structures of (A) the 2,3-pentasaccharide cross-linked lattice with SBA and (B) the 3,6-pentasaccharide cross-linked lattice with SBA. The views are in the *z* plane perpendicular to a 2-fold axis of the tetramer. Protein molecules are shown as trace models and the cross-linking oligosaccharides as CPK models (the aglycon moiety is not shown). One SBA tetramer in the middle of each structure (shown as yellow, magenta, green, and red trace models) is cross-linked by four pentasaccharide molecules to four SBA monomers (shown in aqua) which are part of adjacent tetramers (not shown). One arm of a pentasaccharide molecule binds to the carbohydrate binding site on each subunit of a tetramer and cross-links to a neighboring tetramer by binding to the corresponding site on another monomer. These figures were generated with the program O.

study confirms these observations. Since the structure of SBA itself does not significantly change in the four different complexes (cf. Figure 2), differences in the respective lattice structures of the lectin are due to differences in the structures of the cross-linking carbohydrates. These results clearly demonstrate that the molecular basis for the formation of homogeneous carbohydrate−protein cross-linked complexes between SBA and the four isomeric carbohydrates in Figure 1 is crystal packing interactions that are unique in each cross-linked complex. Thus, the individual structures of the carbohydrates and protein are important structural determinants in the respective cross-linked lattices.

Conclusions. The present findings provide a molecular basis for a new source of specificity in multivalent carbohydrate−lectin interactions, namely, the formation of unique homogeneous cross-linked lattices between multivalent carbohydrates and lectins. The present X-ray data demonstrate that the cross-linked complexes formed between a series of structurally related divalent carbohydrates and a single tetravalent lectin are structurally distinct due to crystal packing interactions. These results confirm and extend quantitative precipitation and electron microscopy experiments which suggested that SBA formed a unique cross-linked lattice with these carbohydrates (*24*).

Importantly, since the driving force for the formation of homoaggregates of multivalent lectins with carbohydrates is solely thermodynamic, other multivalent ligand−macromolecular systems must possess similar properties. The only requirement is that the valency of one of the two interacting molecules must be greater than 2 so that two- or three-dimensional noncovalent cross-linked lattices form and

Scheme 1

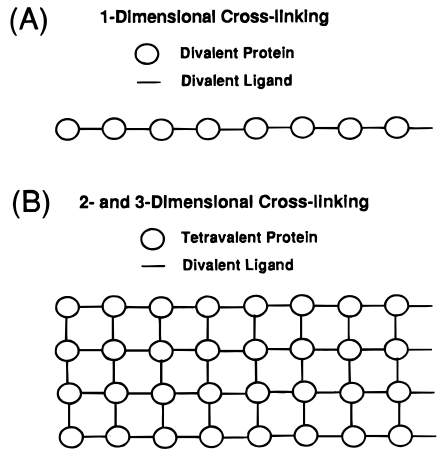

crystalline-type packing constraints can exist (Scheme 1B). Each lattice is thus different for each pair of interacting molecules. In contrast, divalent−divalent protein−ligand interactions give rise to one-dimensional cross-linked complexes which can lead to the formation of heterogeneous aggregation (Scheme 1A).

Lectin−carbohydrate cross-linking interactions have been shown to be important in cellular recognition and signal transduction processes in both plants and animals. The present results together with studies of lectin−glycoprotein interactions (cf. ref 40) indicate that the carbohydrate moieties of specific glycoconjugate receptors can be cross-linked by a multivalent lectin into distinct homogeneous complexes. These individual, segregated complexes may have unique signal transduction properties, for example, in

the immunomodulatory activities of lectins via activation of the T-cell receptor and its closely associated proteins by lectins such as ConA and SBA (cf. ref 41). The crystal structures of the four SBA−pentasaccharide complexes thus represent models for lectin−carbohydrate multidimensional clustering *in vivo* and a common thermodynamic mechanism for selectively aggregating a dispersed population of multivalent receptors in biological systems.

REFERENCES

1. Sharon, N., and Lis, H. (1993) *Scientific Am. 268 (1)*, 82−89.
2. Rini, J. M. (1995) *Annu. Rev. Biophys. Biochem. 24*, 551−577.
3. Kasai, K.-i., and Hirabayashi, J. (1996) *J. Biochem. 119*, 1−8.
4. Drickamer, K., and Taylor, M. E. (1993) *Annu. Rev. Cell Biol. 9*, 237−264.
5. Lotan, R., and Raz, A. (1988) *Ann. N.Y. Acad. Sci. 551*, 385−398.
6. Konstantinov, K. N., Robbins, B. A., and Liu, F.-T. (1996) *Am. J. Pathol. 148*, 25−30.
7. Perillo, N. L., Pace, K. E., Seilhamer, J. J., and Baum, L. G. (1995) *Nature 378*, 736−739.
8. Drickamer, K. (1995) *Nat. Struct. Biol. 2*, 437−439.
9. Nicolson, G. L. (1976) *Biochim. Biophys. Acta 457*, 57−108.
10. Edmonds, B. T., and Koenig, E. (1990) *Cell Motil. Cytoskeleton 17*, 106−117.
11. Kooijman, R., de Wildt, P., van der Bliet, G., Homan, W., Kalshoven, H., Musgarave, A., and van der Ende, H. (1989) *J. Cell Biol. 109*, 1677−1687.
12. Chung, K.-N., Walter, P., Aponte, G. W., and Moore, H.-P. (1989) *Science 243*, 192−197.
13. Carraway, K. L., and Carraway, C. A. C. (1989) *Biochim. Biophys. Acta 988*, 147−171.
14. Edelman, G. M. (1976) *Science 192*, 218−226.
15. Bhattacharyya, L., Ceccarini, C., Lorenzoni, P., and Brewer, C. F. (1987) *J. Biol. Chem. 262*, 1288−1293.
16. Bhattacharyya, L., Haraldsson, M., and Brewer, C. F. (1987) *J. Biol. Chem. 262*, 1294−1299.
17. Bhattacharyya, L., Haraldsson, M., and Brewer, C. F. (1988) *Biochemistry 27*, 1034−1041.
18. Bhattacharyya, L., Haraldsson, M., Sharon, N., Lis, H., and Brewer, F. (1989) *Glycoconjugate J. 6*, 141−150.
19. Bhattacharyya, L., and Brewer, C. F. (1989) *Eur. J. Biochem. 178*, 721−726.
20. Bhattacharyya, L., Fant, J., Lonn, H., and Brewer, C. F. (1990) *Biochemistry 29*, 7523−7530.
21. Bhattacharyya, L., Khan, M. I., and Brewer, C. F. (1988) *Biochemistry 27*, 8762−8767.
22. Bhattacharyya, L., Khan, M. I., Fant, J., and Brewer, C. F. (1989) *J. Biol. Chem. 264*, 11543−11545.
23. Bhattacharyya, L., and Brewer, C. F. (1992) *Eur. J. Biochem. 208*, 179−185.
24. Gupta, D., Bhattacharyya, L., Fant, J., Macaluso, F., Sabesan, S., and Brewer, C. F. (1994) *Biochemistry 33*, 7495−7504.
25. Dessen, A., Gupta, D., Sabesan, S., Brewer, C. F., and Sacchettini, J. C. (1995) *Biochemistry 34*, 4933−4942.
26. Sabesan, S., Duus, J. O., Neira, S., Domaille, P., Kelm, S., Paulson, J. C., and Bock, K. (1992) *J. Am. Chem. Soc. 114*, 8363−8375.
27. Howard, A. J., Gilliland, G. L., Finzel, B. C., Poulos, T. L., Ohlendorf, D. H., and Salemme, F. R. (1987) *J. Appl. Crystallogr. 20*, 383−387.
28. Brunger, A. T. (1990) *X-PLOR Version 3.1 Manual*, Yale University Press, New Haven, CT.
29. Jones, T. A. (1985) *Methods Enzymol. 115*, 157−171.
30. Tronrud, D., Ten Eyck, L., and Matthews, B. (1988) *Acta Crystallogr., Sect. A 43*, 489.
31. Reeke, G. N., Jr., and Becker, J. W. (1986) *Curr. Top. Microbiol. Immunol.* 139, 35−58.
32. Hamelryck, T. W., Dao-Thi, M.-H., Poortmans, F., Chrispeels, M. J., Wyns, L., and Loris, R. (1996) *J. Biol. Chem. 271*, 20479−20485.
33. Navaza, J. (1994) *Acta Crystallogr., Sect. A 50*, 157−163.
34. Jones, T. A., Zou, J. Y., Cowan, S. W., and Kjeldgaard, M. (1991) *Acta Crystallogr., Sect. A 47*, 110−119.
35. Einspahr, H., Parks, E. H., Suguna, K., Subramanian, E., and Suddath, F. L. (1986) *J. Biol. Chem. 261*, 349−361.
36. Liao, D.-I., Kapadia, G., Ahmed, H., Vatsa, G. R., and Herzberg, O. (1994) *Proc. Natl. Acad. Sci. U.S.A. 91*, 1428−1432.
37. Imberty, A., Delage, M.-M., Bourne, Y., Cambillau, C., and Perez, S. (1991) *Glycoconjugate J. 8*, 456−483.
38. Bock, K., Duus, J. O., Hindsgaul, O., and Lindh, I. (1992) *Carbohydr. Res. 228*, 1−20.
39. Bourne, Y., Bolgiano, B., Liao, D.-l., Strecker, G., Cantau, P., Herzberg, O., Feizi, T., and Cambillau, C. (1994) *Nat. Struct. Biol. 1*, 863−870.
40. Brewer, C. F. (1997) *Trends Glycosci. Glycotechol. 9*, 155−165.
41. Liscastro, F., Davis, L. J., and Morini, M. C. (1993) *Int. J. Biochem. 25*, 845−852.

BI971828+